HHS Public Access

Author manuscript

J Thromb Haemost. Author manuscript; available in PMC 2018 April 01.

Published in final edited form as:

J Thromb Haemost. 2017 April ; 15(4): 792–801. doi:10.1111/jth.13619.

Dysregulation of *PLDN* (Pallidin) is a mechanism for platelet dense granule deficiency in *RUNX1* haplodeficiency

G.F. Mao, M.D.[*], **L.E. Goldfinger, Ph.D.**[*,‡], **D.C. Fan, M.D., Ph.D.**[*], **M. P. Lambert, M.D., M.T.R.**[¶,**], **G. Jalagadugula, Ph.D.**[*], **R. Freishtat, M.D.**[§], and **A. K. Rao, M.B.B.S.**[*,†]

[*]Sol Sherry Thrombosis Research Center, Temple University School of Medicine, Philadelphia, PA

[†]Department of Medicine, Temple University School of Medicine, Philadelphia, PA

[‡]Department of Anatomy and Cell Biology, Temple University School of Medicine, Philadelphia, PA

[§]Department of Pediatrics, Children's National Medical Center, Washington, DC

[¶]Division of Hematology, Children's Hospital of Philadelphia, Perelman School of Medicine at the University of Pennsylvania

[**]Department of Pediatrics, Perelman School of Medicine at the University of Pennsylvania

Summary

Background—Inherited *RUNX1* haplodeficiency is associated with thrombocytopenia and platelet dysfunction. Dense granule (DG) deficiency is reported in patients with *RUNX1* haplodeficiency, but the molecular mechanisms are unknown. Platelet mRNA expression profiling in a patient previously reported by us with a *RUNX1* mutation and platelet dysfunction showed decreased expression of *PLDN (BLOC1S6),* which encodes for pallidin, a subunit of BLOC-1 (*b*iogenesis of *l*ysosome-*r*elated *o*rganelles *c*omplex-1) involved in granule biogenesis. *PLDN* mutations in the pallid mouse and the Hermansky-Pudlak syndrome (HPS)-9 are associated with platelet DG deficiency.

Objectives—We postulated that *PLDN* is a RUNX1 target and that its decreased expression leads to platelet DG deficiency in *RUNX1* haplodeficiency.

Results—Platelet pallidin and DG were decreased in our patient. This was also observed in two siblings from a different family with a *RUNX1* mutation. Chromatin immunoprecipitation and electrophoretic mobility shift assays using phorbol ester-treated human erythroleukemia (HEL)

Address correspondence to A. Koneti Rao, M.B.B.S., Sol Sherry Thrombosis Research Center, Hematology Division, Temple University School of Medicine, 3400 N. Broad St., MRB 204, Philadelphia, PA 19140, 215-707-4684 (phone), 215-707-2783 (fax), koneti@temple.edu.

Addendum

G. F. Mao performed the research, analyzed and interpreted data, and contributed to the drafting of the paper; L. E. Goldfinger designed and performed the research, analyzed and interpreted the data, and contributed to the drafting and review of the manuscript; M. P. Lambert characterized the platelet defects and the RUNX1 mutation in two of the patients studied; D. C. Fan and G. Jalagadugula performed the research; R. Freishtat performed the research and contributed to discussion of results; A. K. Rao conceived, designed and performed research, interpreted data, and wrote the paper. All authors have read and approved the manuscript.

Disclosure of Conflict of Interests

The authors state that they have no conflict of interest.

cells showed RUNX1 binding to RUNX1 consensus sites in the *PLDN1* 5′ upstream region. In luciferase reporter studies, mutation of RUNX1 sites in the *PLDN* promoter reduced activity. *RUNX1* over-expression enhanced and *RUNX1* downregulation decreased *PLDN1* promoter activity and protein expression. *RUNX1* downregulation resulted in impaired handling of mepacrine and mislocalization of DG marker CD63 in HEL cells, indicating impaired DG formation, with recapitulation of findings on *PLDN* downregulation.

Conclusions—These studies provide the first evidence that *PLDN* is a direct target of RUNX1 and its dysregulation is a mechanism for platelet DG deficiency associated with *RUNX1* haplodeficiency.

Keywords

Blood Platelets; RUNX1; PLDN protein; human; Platelet Storage Pool Deficiency; thrombocytopenia

Introduction

Mutations in transcription factors, particularly *RUNX1*, are being recognized more frequently as the genetic basis of platelet dysfunction in patients with bleeding disorders [1–3]. RUNX1 haplodeficiency is associated with familial thrombocytopenia, impaired platelet function and megakaryopoiesis, and a predisposition to acute leukemia [2, 4]. Several platelet abnormalities are reported in patients with *RUNX1* mutations, including impaired aggregation, secretion, and protein phosphorylation, and storage pool deficiency (SPD) [2, 5–7].

Platelet granule deficiency leading to impaired platelet function is an important abnormality associated with RUNX1 mutations [2, 5]. In 1969, Weiss and colleagues [8] described a family with inherited platelet dysfunction due to reduced platelet ADP and ATP, indicating a dense granule (DG) SPD. This affected family, and some of the others described with deficiencies of DG or α-granules, have been subsequently shown to carry *RUNX1* mutations [6, 9, 10]. In studies using targeted high throughput sequencing some patients considered to have DG-SPD were found to have *RUNX1* mutations [11]. Moreover, Connelly and colleagues [10] differentiated induced pluripotent stem cells (iPSCs) from skin fibroblasts of two patients with *RUNX1* mutations and showed abnormalities in megakaryocyte production and structure, including a DG deficiency. Targeted *in vitro* correction of *RUNX1* mutation could recover the megakaryocyte defects, providing evidence that *RUNX1* mutation was the cause. The mechanisms leading to the DG deficiency in patients with *RUNX1* mutations are unknown. In general, platelet DG deficiency may arise by multiple mechanisms and be associated with granule abnormalities in other cells (such as melanocytes and neurons) as occurs in the Hermansky-Pudlak syndrome (HPS) [12, 13].

We have reported detailed studies in a patient with inherited heterozygous *RUNX1* mutation, thrombocytopenia and abnormal platelet function [14, 15]. The platelet abnormalities included impaired agonist-induced aggregation, DG secretion, myosin light chain and pleckstrin phosphorylation, and decreased platelet PKC-θ. Platelet mRNA expression profiling showed downregulation of several genes, including *MYL9*, *PF4* and *ALOX12,* and

we have shown that these are direct transcriptional targets of RUNX1 [2, 16–19]. In addition, platelet expression of *PLDN* (pallidin) was downregulated 4-fold (fold change 0.239, $p < 0.029$) in the patient [20].

PLDN, which encodes for a 172-amino acid protein [21] and is linked to granule biogenesis. It is mutated in the naturally occurring mouse model of HPS (the pallid mouse) [21], and is associated with DG deficiency and a pigmentary disorder. More recently, a homozygous *PLDN* mutation has been reported in a patient with the HPS-9 [22]. Pallidin is one of 8 subunits that constitute the BLOC-1 (biogenesis of lysosome-related organelles complex-1), which plays a major role in granule/vesicle biogenesis [13]. Human *PLDN* has two known transcripts; PLDN1 is expressed ubiquitously, while PLDN2 is expressed in brain, testes and leukocytes [21]. Because of the association of platelet DG deficiency with *PLDN* abnormalities [21, 22] and the DG deficiency observed in patients with *RUNX1* mutations [2, 5], we postulated that *PLDN* is a direct transcriptional target of RUNX1 and that its decreased expression may constitute a mechanism for the granule defect. Here we present the first evidence that *PLDN* is a direct transcriptional target of RUNX1, and that RUNX1 or pallidin downregulation is associated with altered DG biogenesis. These studies provide a mechanism involving pallidin for the DG deficiency associated with human *RUNX1* mutations.

Materials and Methods

Patient Information

We have previously described [14, 15, 20] the clinical presentation and studies in a 33-year-old white male, documenting mild thrombocytopenia with decreased agonist-stimulated platelet aggregation, secretion, GPIIb-IIIa activation, and phosphorylation of pleckstrin and myosin light chain (MLC); platelet PKC-θ level was also decreased. The patient has a single point mutation in *RUNX1*, in intron 3 at the splice acceptor site for exon 4, leading to a frameshift and premature termination in the Runt domain [15].

We report here studies in two additional patients (8 years, male, and 3 years, female) with thrombocytopenia and a *RUNX1* mutation (c.508+1G>1). The maternal grandmother and great uncle had history of acute myeloid leukemia. The male subject has had abnormal platelet function on laboratory testing.

This research was approved by the institutional human subjects review board and all participants gave written informed consent.

Materials

The *RUNX1* siRNA, *PLDN* siRNA, control siRNA and antibodies against RUNX1, CD63, cappuccino and β-actin and pre-immune IgG were purchased from Santa Cruz Biotechnology (Santa Cruz, CA). Antibodies against pallidin were purchased from Abnova (Taipei, Taiwan). Antibodies against snapin were from Proteintech Group, Inc (Rosemont, IL). Phorbol 12-myristate 13-acetate (PMA) was from Enzon Life Sciences (Farmingdale, NY). Mepacrine (quinacrine, dihydrochloride) was from EMD Millipore Corporation (Temecula, CA). Luciferase Reporter Assay System kit, PCR reagents, PGL3-basic vector,

and the *Renilla* luciferase control vector were purchased from Promega Biotech (Madison, WI). TRIzol reagent was from Invitrogen (Carlsbad, CA). All oligonucleotides and IRDye-labeled probes were synthesized by Integrated DNA Technologies, (Coralville, IA). Fluorophore-conjugated secondary antibodies raised in donkey were from Jackson ImmunoResearch Laboratories (West Grove, PA).

Preparation of platelet RNA and proteins

Whole blood samples (42.5 ml) were collected from the subjects into 7.5 ml each of acid citrate dextrose (ACD) solution (71.4 mm citric acid, 85 mM sodium citrate-dihydrate, 11.1 mM dextrose) as described previously[20]. The platelet pellet washed twice in Hepes buffer (pH 6.5, 20 mM Hepes, 5.5 mM dextrose, 0.376 mM NaH_2PO_4, 1 mM $MgCl_2$ 2.7 mM KCl, 137 mM NaCl and 1 mg/ml bovine serum albumin). Platelet pellets were resuspended in TRIzol Reagent (Invitrogen, Carlsbad, CA) for total RNA isolation as recommended by the manufacturer. For preparing platelet protein, pellets were resuspended in M-Per Mammalian Protein Extraction Reagent (ThermoFisher Scientific, Grand Island, NY) with proteinase inhibitors. Samples were stored at −80°C.

HEL Cell Culture

Human erythroleukemia (HEL) cells obtained from the American Type Culture Collection (Rockville, MD) were cultured in RPMI 1640 medium (Cellgro) supplemented with 10% fetal bovine serum (FBS) (GE Healthcare, Mississauga, Canada) and penicillin/streptomycin (100 U/ml/100 mg/ml, Invitrogen) at 37°C in a humidified 5% CO_2 atmosphere. HEL cells were treated with 30 nM phorbol myristate acetate (PMA) to induce megakaryocytic transformation.

Chromatin Immunoprecipitation (ChIP) Assays

HEL cells treated with PMA (30 nM) were cross-linked with 1% formaldehyde. ChIP analysis was performed using the Active Motif ChIP assay kit (Carlsbad, CA). Chromatin was immunoprecipitated using anti-RUNX1 antibodies and control IgG (Santa Cruz, sc-2027). PCR reactions were performed to detect the RUNX1 site binding (primers listed in Supplemental Table 1). As controls, PCR was performed on the genomic DNA from the initial sample and on the solubilized cross-linked chromatin prior to immunoprecipitation (input DNA). PCR products were analyzed by electrophoresis on 1% agarose gels.

Electrophoretic mobility shift assay

Nuclear protein was extracted from PMA (30 nM)-treated HEL cells using NE-PER Nuclear and Cytoplasmic Extraction Reagents (ThermoFisher). IRDye-labeled oligonucleotides (IDT) were double-stranded. 10 μg of nuclear protein was incubated with 0.2 ng of labeled probe, and 1 μg of Poly dI-dC in a 15 μl reaction, containing 10% glycerol, 20 mM HEPES, 30 mM KCl, 30 mM NaCl, 3 mM $MgCl_2$, 1 mM DTT (dithiothreitol), for 10 min at room temperature (~22°C) and 10 min on ice before analysis on 4% polyacrylamide gels run at 4°C. For super-shift assays, 1 μg of anti-RUNX1 antibodies or control IgG was incubated with the nuclear extract for 10 min at room temperature before addition of IRDye-labeled probe. Competition assays were carried out by addition of 200-fold excess unlabeled probe

at stated concentrations in 2 μl of nuclear extract and incubated for 10 min on ice before addition of labeled probe. The oligonucleotide sequences used to prepare DNA probes with the binding sites are shown in Supplemental Table 2.

Promoter and Plasmid Construction

Genomic DNA was isolated from human blood using Genomic DNA isolation kit (Qiagen, Valencia, VA). The promoter region of *PLDN* was obtained by PCR amplification of genomic DNA with the primers listed in Supplemental Table 3. Promoter-luciferase constructs were generated with DNA fragments containing human *PLDN* promoter regions −2288 to −23, and −105 to −23 (from ATG) and cloned into the PGL3-basic vector (Promega, Madison, WI). The constructs with RUNX1 sites mutated were generated using the Quick Change Site-Directed system (Stratagene Inc., La Jolla, CA) (Supplemental Table 3).

Luciferase reporter assay

HEL cells were grown in 24-well plates and treated with 30 nM PMA. Transfections were performed using Lipofectamine™ 2000 Reagent (Invitrogen, Carlsbad, CA). Cells (2×10^5) were co-transfected with 200 ng of either the empty PGL3-basic plasmid (Promega, Madison, WI) or PGL3-basic plasmid containing the *PLDN* promoter region, and 10 ng of pRL-TK vector DNA (Promega). The pRL-TK vector, which provided constitutive expression of *Renilla* luciferase, was co-transfected as an internal control. Cells were analyzed at 24 or 48 hours for luciferase activity using the Dual Luciferase Reporter Assay system (Promega).

Quantitative Real Time PCR

Total RNA was extracted using TRIzol Reagent (Invitrogen) quantified with NanoDrop (Thermo Scientific). RNA (1 μg) was reverse-transcribed using Superscript III (Applied Biosystems). The resulting cDNA was diluted 1:50 in nuclease-free water for real time PCR reactions. The final concentration of primers in each reaction was 0.1 μM. The PCR parameters were: 95°C for 10 min and 40 cycles of 95°C 15 seconds, 55°C 20 seconds, and 72°C 20 seconds, using a Master Cycler Real-Time PCR System (Eppendorf, Hauppauge, NY), and relative abundances were calculated by the $\Delta\Delta C_T$ method using GAPDH as the reference gene. The forward (F) and reverse (R) primers used are shown in Supplemental Table 4.

Cell extracts and Immunoblotting

Cell extracts lysed with M-Per Protein Extraction Reagent (Pierce) with protease inhibitors (Enzo Life Sciences) were subjected to 10% or 12% SDS-polyacrylamide gel electrophoresis, transferred to PVDF membranes (Millipore, Billerica, MA) and probed with indicated antibodies. Proteins were detected with IRDye-labeled secondary antibodies and the Odyssey Infrared Imaging system (Li-Cor Biosciences). The quantification from the immunoblots was performed using ImageJ software.

siRNA transfection

PLDN promoter plasmid transfection of PMA-treated HEL cells was performed using Lipofectamine 2000 (Invitrogen, Carlsbad, CA). *RUNX1* siRNA or *PLDN* siRNA (50–80 nM), consisting of pools of three 20–25 bp oligonucleotides, or control siRNA (Santa Cruz), were co-transfected with the *PLDN* −2288/PGL3 reporter plasmid using Lipofectamine 2000. Cells were harvested at 24, 48 or 72 hours, and total RNA and cell lysates were prepared for luciferase reporter activity assays, immunoblotting and quantitative RT-PCR. For studies on DG biogenesis HEL cells were cultured for 7 days with PMA; two sequential siRNA transfections were performed on days 1 and 4 [23].

RUNX1 over-expression

The expression plasmid RUNX1-pCMV6-XL4 and empty pCMV6-XL4 vector were obtained from OriGene Technologies (Rockville, MD). HEL cells were co-transfected using Lipofectamine 2000 (Invitrogen) with 1.25 μg of plasmid RUNX1-pCMV6-XL4 or empty vector and *PLDN* promoter luciferase reporter constructs (−2288/PGL3-basic). The cells were harvested at 24 hours for luciferase activity and at 48 hours for immunoblotting or RNA extraction.

Immunostaining and microscopy

Cells were seeded on glass coverslips, fixed, permeabilized, stained with antibodies and mounted on slides as described previously [24]. In some cases, adhered, washed cells were labeled with 10 μM mepacrine for 5 min prior to 3 rapid PBS rinses and immediate fixation [23]. Nuclear staining was with 30 nM 4′,6-diamidino-2-phenylindole (DAPI) for 10 min at RT. Fluorophores used were FITC and Cy3 (Jackson Immunoresearch). Cells were imaged using a Leica DM IRE2 microscope with a TCS SL confocal system, using a 63x/1.40 NA oil immersion objective at room temperature and Leica imaging software, or on a Nikon E800, using a 63x/1.40 NA oil-immersion objective at room temperature and Q-Capture software. Mepacrine fluorescence was visualized using the 488 nm filter cube or laser. Confocal images were captured by line sequential scanning using 4× line averaging and 3× frame averaging at 400 Hz scan speed. Post-acquisition image processing was performed using ImageJ and Adobe Photoshop. Operations included brightness/contrast adjustment to all pixels in the images and grouping of images. Pearson's correlation coefficients were calculated using Leica imaging software. Fluorescence intensity analysis was performed using ImageJ and Microsoft Excel. Corrected total cellular fluorescence was calculated as the average of individual cell fluorescence intensities divided by the single cell area, background subtracted, > 100 cells per sample.

Web Resources

Potential transcription factor RUNX1 binding sites were predicted by use of the TFsearch system (http://www.cbrc.jp/research/db/TFSEARCH.html).

Statistical Analysis

Results are expressed as the mean ±SEM Differences were compared using the Student's *t*-test and considered significant at p values < 0.05.

Results

Platelet pallidin and dense granules are decreased in the patient

Expression profiling of platelets from the patient with *RUNX1* haplodeficiency showed that *PLDN* expression was decreased compared to platelets from normal subjects (fold change 0.239, $p = 0.029$) [20]. This was validated using quantitative PCR: the platelet *PLDN* mRNA in the patient was lower than 4 healthy subjects (Figure 1A). Platelet transcript levels of the other members of the BLOC-1 complex were detected and not decreased [20]. Immunoflourescence studies using anti-pallidin antibodies showed that the corrected total cellular immunofluorescence (CTCF) was reduced by ~ 33% in patient platelets compared to those from a control subject (Figure 1B), indicating decreased pallidin expression. We examined platelet levels of three other members of the BLOC-1 complex, cappuccino (BLOC1S4) and snapin, previously reported to be decreased in a patient with *PLDN* mutation (HPS9) [22], and these were not decreased in the patient (Supplemental Figure 1). Levels of dysbindin linked to HPS7 [13] were also not decreased (not shown). Platelet DG assessed using anti-CD63 (granulophysin) antibodies, a marker for dense granules [25], showed decreased mean number of CD63-positive granules per platelet in the patient compared to the control subject (Figure 1C). The mean number of granules in the control subject was consistent with previous reports [25].

Studies on platelets from two additional patients with *RUNX1* mutation also showed decreased *PLDN* mRNA and protein, as well as decreased dense granules (Figure 2) when compared to healthy controls.

RUNX1 binds to the PLDN promoter region in vivo

Analysis *in silico* revealed 6 RUNX1 consensus binding sites located within 2288 base pairs of the *PLDN* 5′ upstream region from the ATG (Figure 3A). ChIP studies using PMA-treated HEL cells showed enrichment consistent with RUNX1 binding to chromatin at regions encompassing RUNX1 binding sites 1 (−184/−179 bp), 2 (−246/241 bp), 3 (−1370/−1365 bp), 4 (−1689/−1684 bp), and 5 (−2065/−2060 bp) (Figure 3B). In each case, PCR amplification showed enrichment by anti-RUNX1 antibodies, but not control IgG, of the regions encompassing the RUNX1 consensus sites, indicating RUNX1 binding *in vivo* to the *PLDN* promoter at several sites.

RUNX1 binds *PLDN* promoter sequences

EMSA studies using nuclear extracts from PMA-treated HEL cells showed RUNX1 binding to probes containing each of the six consensus sites (Figure 4). In studies with the probe containing site 1 (Figure 4) there was protein binding (Figure 4, Panel 1, lane 2) that was competed with excess unlabeled probe (lane 3), and super-shifted by anti-RUNX1 antibodies (lane 4), but not by non-specific IgG (lane 5), indicating that RUNX1 was a component of the protein-DNA complex. Similarly, in studies with probes containing sites 2 through 6 (Figure 4, Panels 2–6), there was specific protein binding, that was competed by excess unlabeled probe, and one or more bands observed were super-shifted in studies with probes bearing sites 2, 3, 5 and 6 (Figure 4, panels 2, 3, 5 and 6). In studies with the probe with site 4, (Figure 4, panel 4), there was no supershift noted, but the protein binding was competed

by anti-RUNX1 antibodies, but not non-specific IgG. This is consistent with RUNX1 binding to the probe. Together, these studies demonstrate that RUNX1 binds in the regions encompassing several of the RUNX1 consensus sites in the *PLDN* promoter.

RUNX1 binding sites have promoter activity

In luciferase reporter studies in HEL cells, mutation of consensus sites 1–4 and 6 in the *PLDN* promoter region resulted in a 60–70% reduction in the *PLDN* promoter activity (Figure 5), indicating that these sites, excepting site 5, were functional.

RUNX1 modulates PLDN expression and promoter activity

RUNX1 over-expression in HEL cells increased *PLDN* promoter activity, along with an increase in pallidin and RUNX1 mRNA and protein (Figure 6A). The protein levels of RUNX1 and pallidin increased by a mean of 4.3 fold ($p<0.01$) and 75% ($p<0.05$), respectively. (Figure 6A). RUNX1 downregulation using siRNA decreased *PLDN* promoter activity by ~65%, and *RUNX1* and *PLDN* at the mRNA and protein levels (Figure 6B). The protein levels of RUNX1 and pallidin were decreased by a mean of 54% ($p<0.005$) and 29% ($p<0.05$), respectively. *PLDN* downregulation decreased pallidin protein by 65% but not RUNX1 (Figure 6C), indicating that pallidin knockdown does not affect RUNX1 levels. Moreover, there was no decrease in cappuccino or snapin protein (Supplemental Figure 2) or of dysbindin (not shown) on RUNX1 downregulation. Staining with anti-pallidin antibodies showed that the corrected total cellular immunofluorescence was reduced by 51.2% ± 11.1% in RUNX1 siRNA-transfected cells compared to controls (Figure 6D), confirming decreased pallidin protein expression in RUNX1-depleted cells.

RUNXI and PLDN downregulation impairs dense granule biogenesis

Based on known roles of pallidin in DG/vesicle biogenesis, we considered effects of RUNX1 and pallidin depletion on DG biogenesis. Previous studies have shown DG biogenesis in megakaryocytic MEG-01 cells [23]. To evaluate DG biogenesis in HEL cells, we induced megakaryocytic differentiation by treatment with PMA. After 3 day PMA exposure, most cells showed bilobed nuclei, which expanded to multi-lobed nuclei by 7 day PMA exposure (Supplemental Figure 3). We assessed DG in PMA-treated HEL cells using multiple markers. Mepacrine is incorporated by megakaryocytes and platelets into the DG by uptake and is a DG marker [23, 26]. PMA-treated HEL cells showed incorporation of mepacrine into large puncta, which were enriched in both CD63 and Rab7 – two markers for multivesicular bodies and late endosomes that also indicate maturing dense granules [23, 27]. These findings are consistent with the formation of DG in these differentiated HEL cells (Figure 7A). siRNA downregulation of *RUNX1* or *PLDN* decreased mepacrine uptake, displaced CD63 from large puncta, and decreased co-localization of CD63 with mepacrine, indicating a reduction in DG in these cells (Figure 7B, C). Rab7 enrichment in these large puncta was also lost on knockdown of *RUNX1* or *PLDN* (Supplemental Figure 4). The findings with *RUNX1* downregulation were similar to those with downregulation of *PLDN*, a member of BLOC-1 complex implicated in DG biogenesis. Together, these findings with mepacrine, CD63 and Rab7 are consistent with dysregulated DG biogenesis by downregulation of *RUNX1* or *PLDN*. Downregulation of either *RUNX1* or *PLDN* did not alter levels CD63 protein by immunoblotting (Figure 7D) or mRNA (not shown), indicating

that CD63 is not a target of RUNX1, and consistent with the conclusion that loss of functional RUNX1 or pallidin leads to disrupted CD63 trafficking rather than a decrease in CD63 protein synthesis.

Discussion

PLDN downregulation provides a cogent mechanism for the DG deficiency associated with *RUNX1* mutations. Our studies show that platelet pallidin expression was decreased in the patient with *RUNX1* haplodeficiency, along with a decrease in DG, as shown using the DG marker CD63 [25] (Figure 1). This is corroborated by studies in 2 siblings of an unrelated family with *RUNX1* mutation (Figure 2). Platelet DG deficiency is reported in patients with *RUNX1* mutations, and some patients with a DG deficiency have subsequently been shown to have a *RUNX1* mutation [2, 5, 6, 11]. Pallidin deficiency by homozygous mutation in *PLDN* is associated with platelet DG deficiency in the pallid mouse [21] and in human HPS-9 [22]. Pallidin is one of eight proteins constituting the BLOC-1 complex involved in granule biogenesis [13]; of these eight, platelet transcript levels of only *PLDN* were significantly decreased in our patient [20]. At the protein level, we found platelet cappuccino, snapin, (Supplemental Figure 1) and dysbindin, three other members of the BLOC-1 complex, were not decreased suggesting that RUNX1 is not a master transcriptional regulator of all members of this complex. Our studies provide evidence that *PLDN* is a direct transcriptional target of RUNX1, and is regulated by RUNX1 in megakaryocytic cells. We provide evidence that RUNX1 binds to the *PLDN* promoter (Figures 3 and 4), and the reporter gene expression studies demonstrate that the sites have promoter activity (Figure 5). Over-expression of RUNX1 increased pallidin expression and *PLDN* promoter activity (Figure 6). RUNX1 downregulation elicited the opposite effects (Figure 6). These findings provide a mechanism for the decreased platelet *PLDN* mRNA expression in our patient.

Platelet DG were decreased in patient's platelets in studies using CD63 as a marker (Figure 1C). Our studies also suggest that CD63 is not a transcriptional target of RUNX1; platelet CD63 transcript levels were not decreased in the patient, and HEL cell CD63 protein was not decreased with *RUNX1* or *PLDN* downregulation (Figure 7D). Thus, the downregulation of CD63 by *RUNX1* haplodeficiency is not the cause of the granule defect. In HPS patients also cellular *CD63* gene expression was normal [28].

In HEL cells, localization of the DG membrane protein CD63 was altered on *RUNX1* downregulation (Figure 7B,C). Similar effects were observed with *PLDN* knockdown (Figure 6B,C), suggesting that CD63 mislocalization with *RUNX1* knockdown reflected pallidin downregulation. Previous studies have shown that the BLOC-1 complex, which includes pallidin, is required for cargo-specific sorting from vacuolar early endosomes towards mature vesicles, which include DG and melanosomes [29, 30]. Deficiency of BLOC-1 components as occurs in the HPS patients [22, 31, 32] or following knockdown in fibroblasts or melanocytes results in altered distribution of the specific lysosome-related organelles cargo [29, 30]. Specifically, downregulation of pallidin has been shown to result in mislocalization of CD63 in fibroblasts and of tyrosine-receptor related protein TYRP1 (a granule marker) in melanocytes [22, 29, 30]. Our findings on downregulation of *RUNX1* or

PLDN in HEL cells are similar (Figure 7) and recapitulate these reported findings. Moreover, defects noted under these conditions in the retention of mepacrine (Figure 7), which is normally incorporated rapidly into the DG, indicate that RUNX1 regulates DG biogenesis in part through pallidin. The displacement of CD63 from DG by *RUNX1* or *PLDN* knockdown, which did not suppress CD63 expression (Figure 7D), suggests possible repurposing of cargo away from DG and towards other pathways in RUNX1- or pallidin-depleted cells [23]. The fate of CD63 needs to be established in future studies. Overall, the studies with two independent markers - CD63 and mepacrine, provide strong support to the concept that pallidin downregulation alters DG biogenesis and is a potential mechanism for DG deficiency in *RUNX1* haplodeficiency. It is important to note that the patient reported with HPS-9 had a homozygous mutation in *PLDN* [22] and it is unclear if heterozygotes have a subtle granule abnormality in platelets or melanosomes. Based on the magnitude of decrease in pallidin noted in our patients, we postulate that the dense granule deficiency results from a combined effect of decreased expression of *PLDN* and of other genes that are RUNX1 targets and involved in vesicle trafficking [20]. The latter would encompass genes such Rab proteins and others implicated in vesicle transport, as well as yet unknown genes involved in granule biogenesis and regulated by RUNX1 [20].

The DG defect alone does not account for all aspects of the platelet dysfunction noted in RUNX1 haplodeficiency. As previously shown by us [20], several genes are downregulated in *RUNX1* haplodeficiency, indicating that the underpinnings of the platelet dysfunction are complex, involving multiple pathways. Agonist-induced DG secretion is diminished in *RUNX1* haplodeficiency [1, 3, 7, 14], and may be associated with impaired secretion of α–granule contents and acid hydrolases [7]. The decreased DG secretion likely results from abnormalities in the granules *per se* as well as in mechanisms governing secretion, the latter evidenced by documented abnormalities in processes governing exocytosis, including myosin and pleckstrin phosphorylation [14]. Similarly, downregulation of other genes related to vesicle transport [20] may also contribute to defective granule formation and function.

Overall, DG deficiency is one of the major platelet abnormalities reported in patients with RUNX1 mutations [2, 5, 6, 9]. Decreased expression of *PLDN* and associated aberrant granule formation constitutes a cogent mechanism for DG deficiency due to RUNX1 haplodeficiency. Our studies provide new insights into the role of pallidin in granule defects outside of the HPS. The gene dysregulation associated with *RUNXI* haplodeficiency is a valuable model to obtain novel insights into human platelet biology.

Supplementary Material

Refer to Web version on PubMed Central for supplementary material.

Acknowledgments

This study was supported by research funding from NIH (NHLBI) R01HL109568 and R01HL085422 to A. K. Rao, and by AHA 16GRNT27260319 to L. E. Goldfinger.

References

1. Stockley J, Morgan NV, Bem D, Lowe GC, Lordkipanidze M, Dawood B, Simpson MA, Macfarlane K, Horner K, Leo VC, Talks K, Motwani J, Wilde JT, Collins PW, Makris M, Watson SP, Daly ME, Genotyping UK. Phenotyping of Platelets Study G. Enrichment of FLI1 and RUNX1 mutations in families with excessive bleeding and platelet dense granule secretion defects. Blood. 2013; 122:4090–3. [PubMed: 24100448]
2. Songdej N, Rao AK. Hematopoietic transcription factor mutations and inherited platelet dysfunction. F1000prime reports. 2015; 7:66. [PubMed: 26097739]
3. Rao AK. Spotlight on FLI1, RUNX1, and platelet dysfunction. Blood. 2013; 122:4004–6. [PubMed: 24335028]
4. Song WJ, Sullivan MG, Legare RD, Hutchings S, Tan X, Kufrin D, Ratajczak J, Resende IC, Haworth C, Hock R, Loh M, Felix C, Roy DC, Busque L, Kurnit D, Willman C, Gewirtz AM, Speck NA, Bushweller JH, Li FP, et al. Haploinsufficiency of CBFA2 causes familial thrombocytopenia with propensity to develop acute myelogenous leukaemia. Nat Genet. 1999; 23:166–75. [PubMed: 10508512]
5. Rao AK. Inherited platelet function disorders: overview and disorders of granules, secretion, and signal transduction. Hematol Oncol Clin North Am. 2013; 27:585–611. [PubMed: 23714313]
6. Michaud J, Wu F, Osato M, Cottles GM, Yanagida M, Asou N, Shigesada K, Ito Y, Benson KF, Raskind WH, Rossier C, Antonarakis SE, Israels S, McNicol A, Weiss H, Horwitz M, Scott HS. In vitro analyses of known and novel RUNX1/AML1 mutations in dominant familial platelet disorder with predisposition to acute myelogenous leukemia: implications for mechanisms of pathogenesis. Blood. 2002; 99:1364–72. [PubMed: 11830488]
7. Rao AK, Poncz M. Defective platelet secretory mechanisms in familial thrombocytopenia with transcription factor CBFA2 haplodeficiency. Thromb Hemostas. 2001 Abstract #OC91.
8. Weiss HJ, Chervenick PA, Zalusky R, Factor A. A familial defect in platelet function associated with imapired release of adenosine diphosphate. N Engl J Med. 1969; 281:1264–70. [PubMed: 5349805]
9. Weiss HJ, Witte LD, Kaplan KL, Lages BA, Chernoff A, Nossel HL, Goodman DS, Baumgartner HR. Heterogeneity in storage pool deficiency: studies on granule-bound substances in 18 patients including variants deficient in alpha-granules, platelet factor 4, beta-thromboglobulin, and platelet-derived growth factor. Blood. 1979; 54:1296–319. [PubMed: 508939]
10. Connelly JP, Kwon EM, Gao Y, Trivedi NS, Elkahloun AG, Horwitz MS, Cheng L, Liu PP. Targeted correction of RUNX1 mutation in FPD patient-specific induced pluripotent stem cells rescues megakaryopoietic defects. Blood. 2014; 124:1926–30. [PubMed: 25114263]
11. Simeoni I, Stephens JC, Hu F, Deevi SV, Megy K, Bariana TK, Lentaigne C, Schulman S, Sivapalaratnam S, Vries MJ, Westbury SK, Greene D, Papadia S, Alessi MC, Attwood AP, Ballmaier M, Baynam G, Bermejo E, Bertoli M, Bray PF, et al. A high-throughput sequencing test for diagnosing inherited bleeding, thrombotic, and platelet disorders. Blood. 2016; 127:2791–803. [PubMed: 27084890]
12. Seward SL Jr, Gahl WA. Hermansky-Pudlak syndrome: health care throughout life. Pediatrics. 2013; 132:153–60. [PubMed: 23753089]
13. Huizing M, Helip-Wooley A, Westbroek W, Gunay-Aygun M, Gahl WA. Disorders of lysosome-related organelle biogenesis: clinical and molecular genetics. Annual review of genomics and human genetics. 2008; 9:359–86.
14. Gabbeta J, Yang X, Sun L, McLane MA, Niewiarowski S, Rao AK. Abnormal inside-out signal transduction-dependent activation of glycoprotein IIb-IIIa in a patient with impaired pleckstrin phosphorylation. Blood. 1996; 87:1368–76. [PubMed: 8608226]
15. Sun L, Mao G, Rao AK. Association of CBFA2 mutation with decreased platelet PKC-θ and impaired receptor-mediated activation of GPIIb-IIIa and pleckstrin phosphorylation: proteins regulated by CBFA2 play a role in GPIIb-IIIa activation. Blood. 2004; 103:948–54. [PubMed: 14525764]

16. Jalagadugula G, Mao G, Kaur G, Dhanasekaran DN, Rao AK. Platelet PKC-θ deficiency with human RUNX1 mutation: *PRKCQ* is a transcriptional target of RUNX1. Arterioscler Thromb Vasc Biol. 2011:921–7. [PubMed: 21252065]
17. Jalagadugula G, Mao G, Kaur G, Goldfinger LE, Dhanasekaran DN, Rao AK. Regulation of platelet myosin light chain (*MYL9*) by RUNX1: implications for thrombocytopenia and platelet dysfunction in *RUNX1* haplodeficiency. Blood. 2010; 116:6037–45. [PubMed: 20876458]
18. Aneja K, Jalagadugula G, Mao G, Rao AK. Mechanism of platelet factor (PF4) deficiency with RUNX1 mutations: RUNX1 is a transcriptional regulator of PF4. Blood. 2009; 114:98–9.
19. Kaur G, Jalagadugula G, Rao AK. CBFA2/RUNX1 regulates human platelet 12-lipoxygenase: studies in runx1 haplodeficiency. Blood. 2007; 118:1066A.
20. Sun L, Gorospe JR, Hoffman EP, Rao AK. Decreased platelet expression of myosin regulatory light chain polypeptide (MYL9) and other genes with platelet dysfunction and CBFA2/RUNX1 mutation: insights from platelet expression profiling. J Thromb Haemost. 2007; 5:146–54. [PubMed: 17059412]
21. Falcon-Perez JM, Dell'Angelica EC. The pallidin (Pldn) gene and the role of SNARE proteins in melanosome biogenesis. Pigment Cell Res. 2002; 15:82–6. [PubMed: 11936273]
22. Cullinane AR, Curry JA, Carmona-Rivera C, Summers CG, Ciccone C, Cardillo ND, Dorward H, Hess RA, White JG, Adams D, Huizing M, Gahl WA. A BLOC-1 mutation screen reveals that PLDN is mutated in Hermansky-Pudlak Syndrome type 9. Am J Hum Genet. 2011; 88:778–87. [PubMed: 21665000]
23. Ambrosio AL, Boyle JA, Di Pietro SM. Mechanism of platelet dense granule biogenesis: study of cargo transport and function of Rab32 and Rab38 in a model system. Blood. 2012; 120:4072–81. [PubMed: 22927249]
24. Wurtzel JG, Lee S, Singhal SS, Awasthi S, Ginsberg MH, Goldfinger LE. RLIP76 regulates Arf6-dependent cell spreading and migration by linking ARNO with activated R-Ras at recycling endosomes. Biochem Biophys Res Commun. 2015; 467:785–91. [PubMed: 26498519]
25. Nishibori M, Cham B, McNicol A, Shalev A, Jain N, Gerrard JM. The protein CD63 is in platelet dense granules, is deficient in a patient with Hermansky-Pudlak syndrome, and appears identical to granulophysin. J Clin Invest. 1993; 91:1775–82. [PubMed: 7682577]
26. Wall JE, Buijs-Wilts M, Arnold JT, Wang W, White MM, Jennings LK, Jackson CW. A flow cytometric assay using mepacrine for study of uptake and release of platelet dense granule contents. Br J Haematol. 1995; 89:380–5. [PubMed: 7873389]
27. Pols MS, Klumperman J. Trafficking and function of the tetraspanin CD63. Exp Cell Res. 2009; 315:1584–92. [PubMed: 18930046]
28. Armstrong LW, Rom WN, Martiniuk FT. The gene for lysosomal protein CD63 is normal in patients with Hermansky-Pudlak syndrome. Lung. 1998; 176:249–56. [PubMed: 9617741]
29. Setty SR, Tenza D, Truschel ST, Chou E, Sviderskaya EV, Theos AC, Lamoreux ML, Di Pietro SM, Starcevic M, Bennett DC, Dell'Angelica EC, Raposo G, Marks MS. BLOC-1 is required for cargo-specific sorting from vacuolar early endosomes toward lysosome-related organelles. Mol Biol Cell. 2007; 18:768–80. [PubMed: 17182842]
30. Di Pietro SM, Falcon-Perez JM, Tenza D, Setty SR, Marks MS, Raposo G, Dell'Angelica EC. BLOC-1 interacts with BLOC-2 and the AP-3 complex to facilitate protein trafficking on endosomes. Mol Biol Cell. 2006; 17:4027–38. [PubMed: 16837549]
31. Dell'Angelica EC, Shotelersuk V, Aguilar RC, Gahl WA, Bonifacino JS. Altered trafficking of lysosomal proteins in Hermansky-Pudlak syndrome due to mutations in the beta 3A subunit of the AP-3 adaptor. Mol Cell. 1999; 3:11–21. [PubMed: 10024875]
32. Westmoreland D, Shaw M, Grimes W, Metcalf DJ, Burden JJ, Gomez K, Knight AE, Cutler DF. Super-resolution microscopy as a potential approach to diagnosis of platelet granule disorders. J Thromb Haemost. 2016; 14:839–49. [PubMed: 26806224]

Essentials

1. Platelet dense granule (DG) deficiency is a major abnormality in *RUNX1* haplodeficiency patients.
2. The molecular mechanisms leading to the platelet DG deficiency are unknown.
3. Platelet expression of *PLDN* (*BLOC1S6,* pallidin), involved in DG biogenesis, is regulated by RUNX1.
4. Downregulation of *PLDN* is a mechanism for DG deficiency in *RUNX1* haplodeficiency.

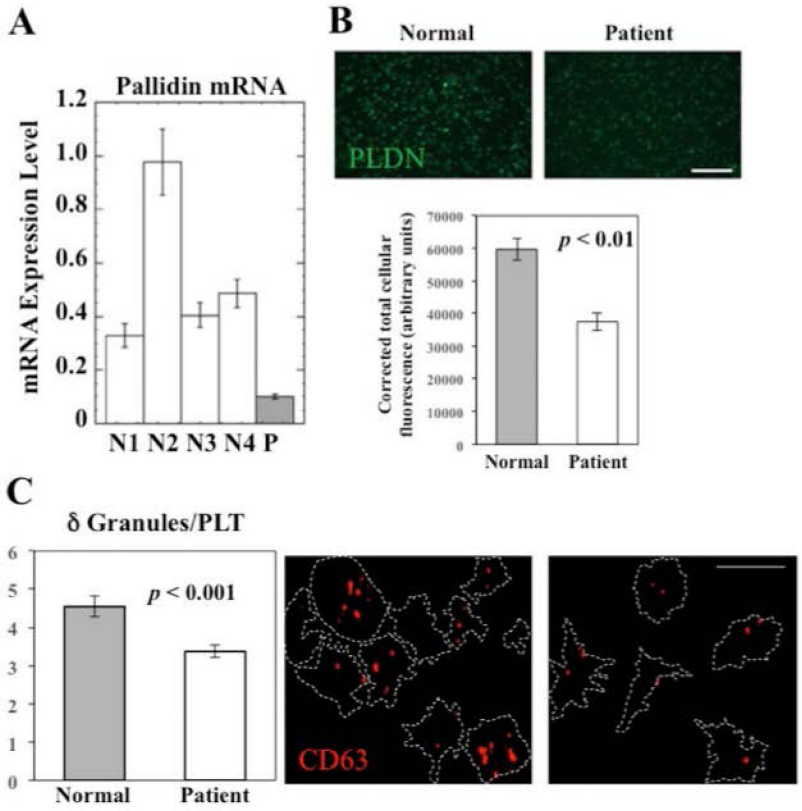

Figure 1. Pallidin (*PLDN*) expression and CD63 positive dense granules in patient platelets

A. Platelets *PLDN* mRNA levels in the patient (P) and four healthy controls (N1–N4) by quantitative PCR. Shown are mRNA levels normalized to GAPDH. B. Pallidin immunostaining (top) and corrected total cellular fluorescence (bottom) in control and patient platelets. Bar, 50 μm. C. Mean CD63-positive granules by immunofluorescence in platelets from the patient and healthy control. Shown are dense granules per platelet (> 100 platelets counted each) from control subject and patient. Bar, 5 μm.

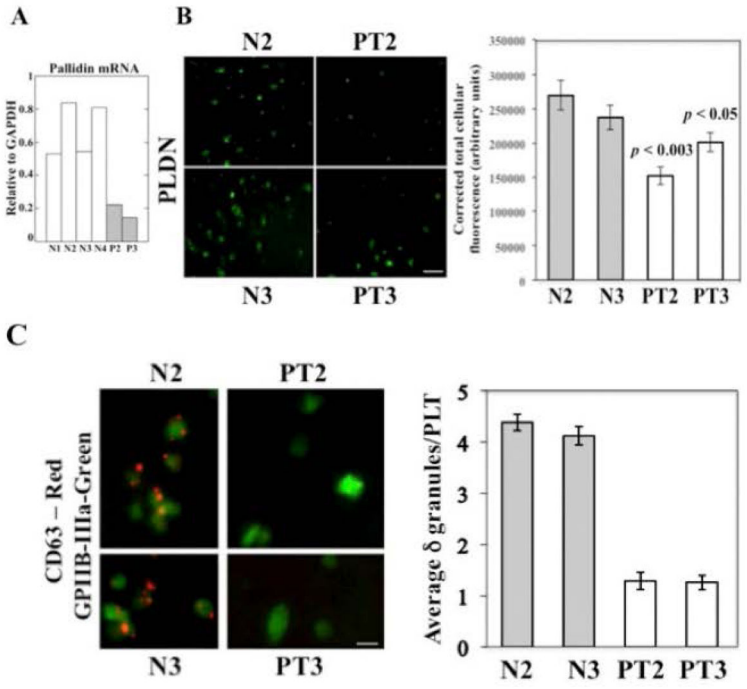

Figure 2. Pallidin (*PLDN*) expression and CD63 positive dense granules in platelets from additional patients with *RUNX1* mutation

Shown are studies in two siblings, brother (patient PT2) and his sister (patient PT3). A. Platelets *PLDN* mRNA levels in the patients (PT2 and PT3) and four healthy controls (N1–N4) by quantitative PCR. Shown are mRNA levels normalized to GAPDH. B. Pallidin immunostaining and corrected total cellular fluorescence of platelets from 2 control subjects (N1 and N2) and the patients (PT2 and PT3). Bar, 50 μm. The p values indicate comparisons of each patient with each of the two control subjects. C. CD63-positive granules by immunofluorescence in platelets from the patients and healthy controls. Shown are mean dense granules per platelet (> 100 platelets counted each) from each subject.. Bar, 5 μm.

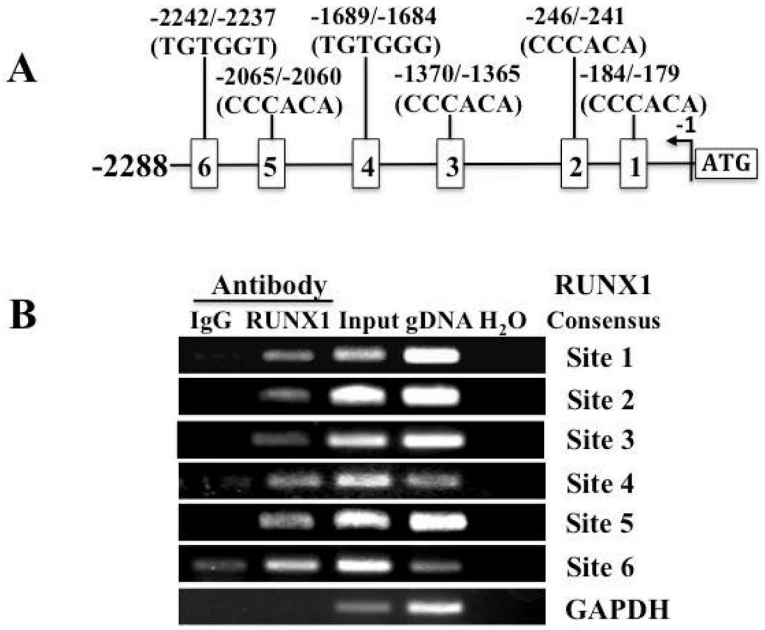

Figure 3. Binding of RUNX1 to *PLDN* promoter region *in vivo* by chromatin immunoprecipitation (ChIP)

The top panel (A) shows the 5′ upstream region of *PLDN* with the putative RUNX1 consensus binding sites. The lower panel shows PCR amplification of the immunoprecipitates with control IgG (column 1) and RUNX1 antibodies (column 2). Columns 3 and 4 show PCR amplification of total input DNA and genomic DNA, respectively. Shown are PCR amplification of *PLDN* promoter regions encompassing RUNX1 binding sites 1–6 and of GAPDH representative of three experiments.

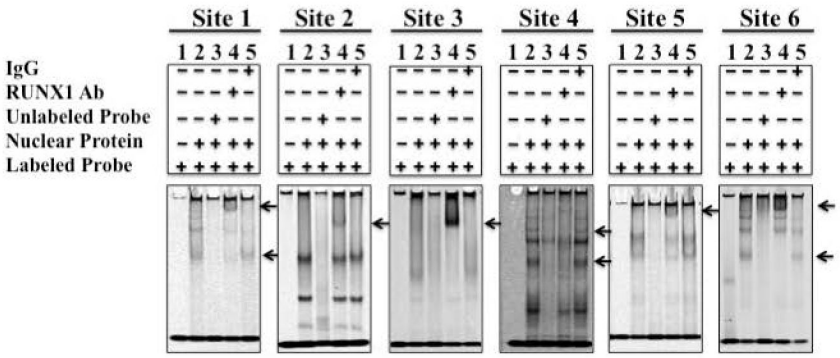

Figure 4. EMSA using oligonucleotide probes with consensus RUNX1 binding sites 1–6 (panels 1–6) and nuclear extract from PMA-treated HEL cells

Details of the location of RUNX1 binding sites 1–6 in the *PLDN* promoter are shown in Figure 2. For each panel, Lane 1: probe alone; lane 2: probe with nuclear extract; lane 3: competition with excess unlabeled probe; lane 4: effect of RUNX1 antibodies; lane 5: effect of pre-immune IgG. The arrows indicate areas where the band was super-shifted or competed by the RUNX1 antibodies. Shown are representative of three experiments with each probe. The nucleotide sequences of the probes are shown in Supplemental Table 2

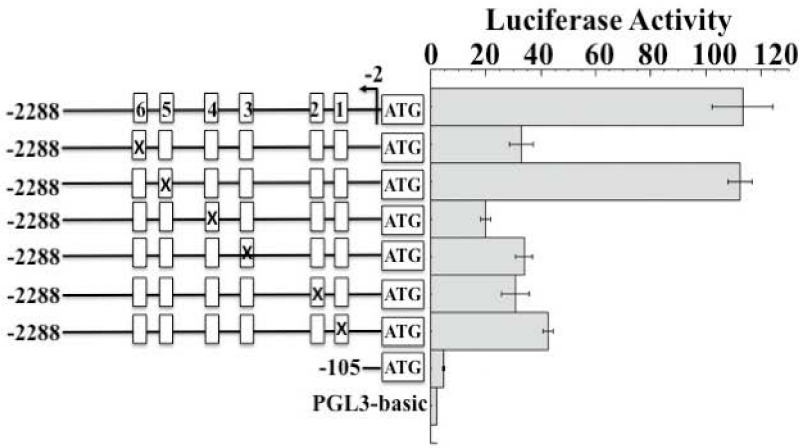

Figure 5. Luciferase reporter studies on the *PLDN* promoter in PMA-treated HEL cells

Shown is luciferase promoter activity at 24 hours of the wildtype construct and the effect of mutating each of the six RUNX1 consensus-binding sites in the 5′ upstream region of *PLDN.* The ratio of firefly to *Renilla* luciferase activity of the wild type construct, constructs with each RUNX1 consensus site mutated, and the vector alone is shown as mean (± SEM) of three experiments.

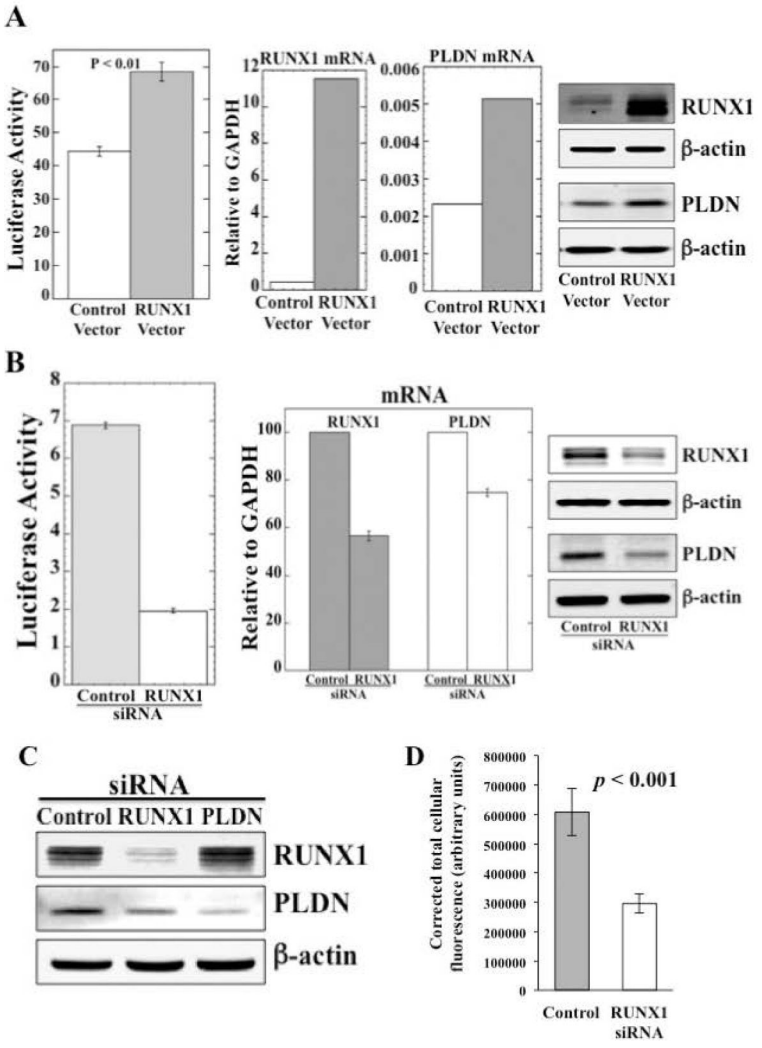

Figure 6. Effects of transient over-expression and siRNA knockdown of RUNX1 on *PLDN* promoter activity and expression

A. Effect of RUNX1 over-expression. HEL cells were co-transfected with *PLDN* luciferase reporter construct (−2288/−2) with or without RUNX1-pCMV6 expression vector. Reporter activity was measured at 24 hours. Bar graphs on the left show activity as mean (±SEM) of three experiments. The bar graphs in the middle show *RUNX1* and *PLDN* mRNA levels. The right panel shows the immunoblots for RUNX1 and pallidin with β-actin as loading control. B. Effect of siRNA *RUNX1* knockdown. HEL cells were co-transfected with *RUNX1* or control siRNA and *PLDN* luciferase-reporter construct (−2288/−2). Bar graphs (left) show promoter activity as mean (±SE) of three experiments. The middle panel shows *RUNX1* and *PLDN* mRNA levels. The right panel shows immunoblots for RUNX1 and pallidin with β-actin as loading control. C. Effect of siRNA *RUNX1* or *PLDN* knockdown on RUNX1 and pallidin protein expression in HEL cells. Immunoblots show protein levels of RUNX1 and pallidin, with β-actin as loading control. D. Corrected total cellular fluorescence following pallidin immunostaining in HEL cells transfected with *RUNX1* or control siRNA.

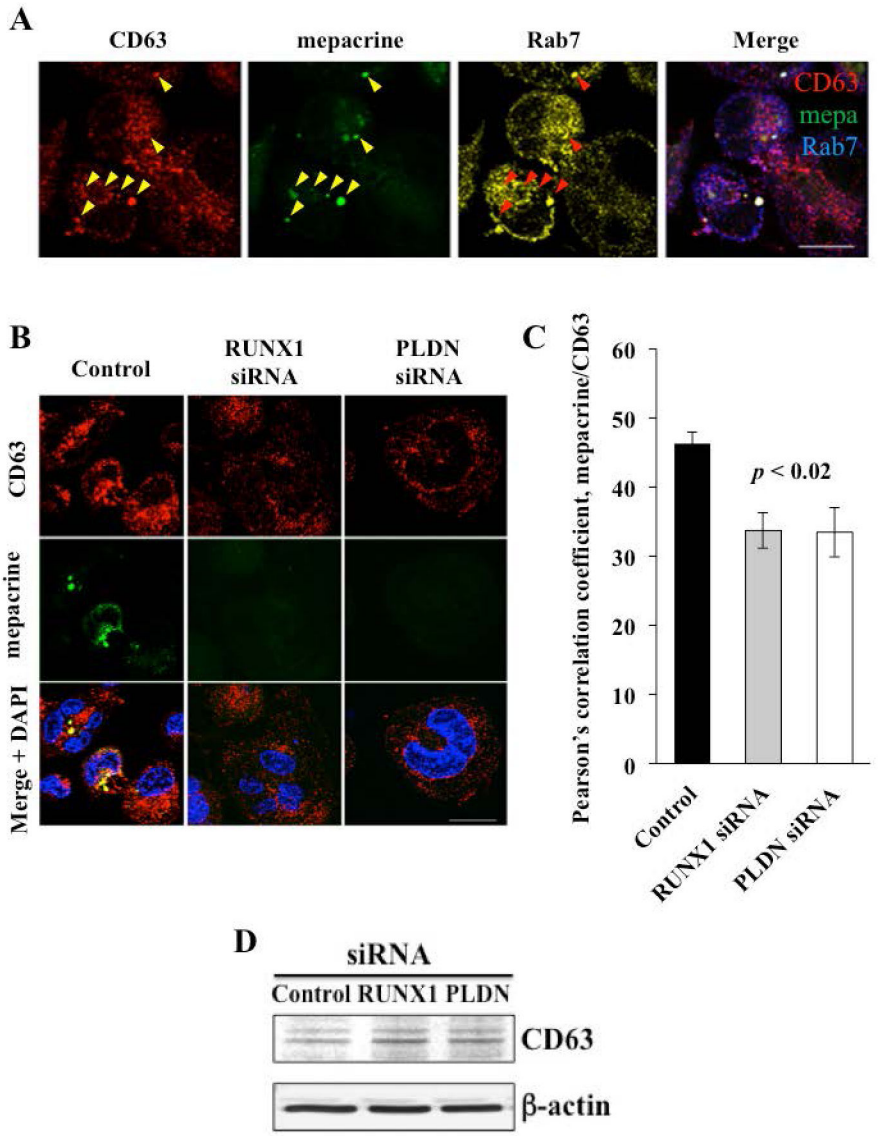

Figure 7. Effects of siRNA knockdown of *RUNX1* and *PLDN* on DG formation, CD63 sub-cellular localization and expression

HEL cells were PMA-treated and incubated with mepacrine as described under Methods. A. Immunostaining of CD63 and Rab7, and mepacrine fluorescence in HEL cells after 7 day PMA treatment. CD63, red; mepacrine, green; Rab7, yellow. Yellow and red arrowheads indicate co-localization in large puncta, which appear as yellow/white in the merged image to the right. Bar, 10 μm. B. HEL cells transfected as indicated were treated with mepacrine, fixed, and stained with antibodies to CD63 and with DAPI. Merged images of CD63 staining and mepacrine and DAPI fluorescence are shown in the bottom row. CD63, red; mepacrine, green; DAPI, blue; mepacrine/CD63 co-localization appears as yellow. Bar, 10 μm. C. Pearson's correlation coefficients for CD63 and mepacrine derived from > 100 cells per sample. D. Immunoblot showing CD63 protein expression in HEL cells transfected with the indicated siRNAs, with β-actin as loading controls.